Submitted to the 30th International Conference on High-Energy Physics ICHEP2000,
Osaka, Japan, July 2000

Rapidity Gaps Between Jets in Photoproduction at HERA

H1 Collaboration

Abstract

Dijet events in photon-proton collisions in which there is a rapidity separation between the two highest E_t jets $\Delta\eta > 2.0$ are studied with the H1 detector at HERA. Jets are defined using the inclusive KT algorithm. Rapidity gap events are defined as events in which the sum of the transverse energy of all jets between the two highest E_t jet axes is less than E_t^{cut} GeV, for $0.5 < E_t^{cut} < 5.0$ GeV. The gap fraction, defined as the fraction of dijet events with a rapidity gap, is plotted for different E_t^{cut} values for the inclusive dijet sample, and differentially in $\Delta\eta$, x_p^{jets}, the fraction of the protons momentum entering the hard scattering and x_γ^{jets}, the fraction of the photons momentum entering the hard scatter . A large excess of events with rapidity gaps at low values of E_t^{cut} is observed above the expectation from standard photoproduction processes. The excess is consistent with the expectation, within the leading logarithmic approximation of BFKL, if high-t pomeron exchange is included.

Abstract: 962
Parallel session: 2
Plenary talk: 12

1 Introduction

Events with large rapidity gaps in the hadronic final state and a perturbatively hard scale at one end of the exchange have long been recognized as a unique place to study the interplay between long and short distance physics. Measurements of diffractive deep inelastic scattering at HERA [1], for example, have led to a phenomenology which mixes the languages of perturbative QCD and Regge theory. A particularly special class of events in which there are hard scales at both ends of the exchange has also been observed at the Tevatron [2, 3] and HERA [4], and is the subject of this study. Such events are characterised by two hard jets in the final state separated by a large rapidity interval and an absence of energy above some small scale between the jets. One might expect to be able to calculate the rate for such a process using only perturbative methods, since the gap producing mechanism is squeezed to small distances [5]. The presence of the rapidity gap coupled with the large rapidity separation of the jets and large momentum transfer means in effect that one is in a perurbatively calculable Regge limit of QCD. This approach is dependent on the construction of a colour singlet object within perturbative QCD, a problem that is far from resolved. Calculations using the leading logarithmic approximation of BFKL [6] have been performed by Mueller and Tang[7] and found to describe the Tevatron gaps between jets data [8] and the related process of high-t vector meson production at HERA [9, 10]. The situation is complicated, however, by the issue of rapidity gap survival probability; interactions, which may be hard or soft, between spectator partons in the colliding hadrons can destroy the gap [11, 12]. This introduces a potentially large non-perturbative component into the calculation of gaps between jets, making absolute predictions of both rates and differential distributions problematic [8]. A related approach which allows a purely perturbative prediction if a dijet gap event is defined in terms of some minimum energy, $Q \gg \Lambda_{QCD}$, between the jets has been developed by Oderda and Sterman [13]. The introduction of a second large scale generates logarithms in the ratio Q/p_t which can be resummed to all orders in perturbation theory. Detailed predictions have been made for dijet photoproduction at HERA, and are in agreement with the published ZEUS data [14]. A different approach which has been found to be equally effective in describing the available data is the 'soft colour rearrangement' or 'colour evaporation' model [15]. In this model, the underlying short distance dynamics is the same for both gap and non-gap dijet events, i.e. predominantly single gluon exchange. The appearance of a rapidity gap is simply the consequence of the exchange of one or many soft gluons which result in the production of colour singlet states at the proton and photon sides of the hard scatter.

The aim of this paper is to measure dijet cross sections and gap fractions differentially in variables which may help to distinguish between competing models of high-t rapidity gap formation.

2 The H1 Detector

A detailed description of the H1 apparatus can be found elsewhere [16]. The following briefly describes the detector components relevant to this analysis.

A liquid argon (LAr) calorimeter [17] covers the range in polar angle $4^\circ < \theta < 153^\circ$ with full azimuthal coverage, where θ is defined with respect to the proton beam direction ($+z$ axis). The LAr consists of an electromagnetic section with lead absorbers and a hadronic section with steel absorbers, of combined depth between 4.5 and 8 interaction lengths. Both sections are highly segmented in the transverse and longitudinal directions with about 44000 cells in total. The absolute energy scale is known to 4% for hadronic energies. The polar region $153^\circ < \theta < 177.8^\circ$ is covered by the SPACAL [18], a lead / scintillating fibre calorimeter with both hadronic and electromagnetic sections. The hadronic energy scale uncertainty is presently 7%. Tracking

Monte Carlo	α_s	Proton PDF	γ PDF	P_t^{min} (GeV)	P_t^{mi} GeV
PYTHIA 5.7	1-loop	GRV-LO	GRV-LO	2.2	1.5
HERWIG 5.9	2-loop	GRV-HO	GRV-HO	2.0	-
HERWIG 5.9 + JIMMY	2-loop	GRV-LO	WHIT-2	1.8	1.8

Table 1: Monte Carlo parameters

information is provided by the two concentric drift chambers of the central tracker, covering the pseudo-rapidity range $-1.5 < \eta < 1.5$, which lie inside a 1.15 T solenoidal field.

The luminosity is measured from the reaction $ep \rightarrow ep\gamma$ with two TlCl/TlBr crystal calorimeters [16] installed in the HERA tunnel. The electron tagger is located at $z = -33$ m from the interaction point in the direction of the outgoing lepton beam and the photon tagger at $z = -103$ m.

3 Simulations

The Pythia 5.7 [19] and Herwig 5.9 [20] Monte Carlo event generators were used to correct the data for detector acceptance and bin migration effects. Both generators simulate the direct and resolved production of dijets by quasi-real photons. The hard scattering matrix elements are calculated to leading order, regulated by a cut-off, P_t^{min}. In addition to the primary hard scatter, the Pythia generator is able to model the effect of multiple parton-parton interactions in a resolved photoproduction event. The probability to have several parton-parton collisions in a single event is modelled using the parton densities and the usual leading order matrix elements [19]. As for the primary hard scatter, the matrix elements are divergent and must be regulated by a cut-off, P_t^{mi}, which is the main free parameter in the model. This parameter was tuned to give the best description of the H1 data, after all kinematic cuts, used in this analysis. [1]. The standard Herwig 5.9 release has a simpler model for multiple interactions which was not used in this analysis as it was found to adversely affect the energy flow in the proton direction, which in turn led to a poor description of the forward jet. A more sophisticated multiple interactions model is now available for Herwig , known as Jimmy . [23]. A sample of Herwig events was generated using Jimmy and used for model comparisons, but was not used for data correction. The main free parameter in the Herwig + Jimmy model is, P_t^{min}, which in the current version of Jimmy must be set equal to P_t^{mi}, the cut off for the matrix elements associated with multiple interactions. Again, this parameter was tuned to give the best description of the H1 data, after all kinematic cuts, used in this analysis. The settings of the above parameters and parton densities used in each of the Monte Carlo simulations are shown in table 1 [2].

Herwig incorporates the BFKL LLA colour singlet exchange cross section for the elastic scattering of two partons as computed by Mueller & Tang [7]

$$\frac{d\sigma(qq \rightarrow qq)}{dt} = \left(\frac{\alpha_s C_F}{\pi}\right)^4 \frac{16\pi^3}{(N_c^2-1)^2}\frac{1}{t^2}\left[\int d\nu \frac{\nu^2}{(\nu^2+1/4)^2} \mathrm{e}^{\omega(\nu)\mathrm{y}}\right]^2 \tag{1}$$

where the leading logarithm BFKL kernel is

$$\omega(\nu) = 2\frac{C_A \alpha_s}{\pi}\mathrm{Re}[\psi(1) - \psi(1/2 + i\nu)] \tag{2}$$

[1] The simplest multiple interaction model in Pythia was used, corresponding to setting switch `MSTP(82)=1`

[2] A global tuning for the Pythia and Herwig + Jimmy generators can be found at http://www.hep.ucl.ac.uk/JetWeb/

and

$$y = \Delta\eta = \ln\left(\frac{\hat{s}}{-t}\right). \tag{3}$$

To this level of accuracy, the jets have equal and opposite transverse momenta, $p_t = \sqrt{-t}$. A version of HERWIG is used in which the right-hand-side of equation (1) is evaluated without approximation [21] [3]. The standard HERWIG 5.9 realease uses the asymptotic approximation also derived in [7]; in the limit $\Delta\eta \gg 1$,

$$\frac{d\sigma(qq \to qq)}{dt} \approx (C_F\alpha_s)^4 \frac{2\pi^3}{t^2} \frac{\exp(2\omega_0 y)}{(7\alpha_s C_A \zeta(3) y)^3} \tag{4}$$

where $\omega_0 = \omega(0) = C_A(4\ln 2/\pi)\alpha_s$. $1 + \omega_0$ is then the hard pomeron intercept. The values of α_s in equations 1 and 2 are free parameters in the LLA, and are chosen[4] to be 0.17. This corresponds to a choice of $\omega_0 = 0.45$. The gluon-quark and gluon-gluon subprocesses are the same as the quark-quark subprocess, up to colour factors, and so the parton level cross-section for the gaps-between-jets process may be written as

$$\begin{aligned} \frac{d\sigma(h_1\ h_2 \to X\ Y)}{dx_1 dx_2 dt} &= \left(\frac{81}{16} g_1(x_1,\mu^2) + \Sigma_1(x_1,\mu^2)\right)\left(\frac{81}{16} g_2(x_2,\mu^2) + \Sigma_2(x_2,\mu^2)\right) \times \\ &\quad \frac{d\sigma(qq \to qq)}{dt} \end{aligned} \tag{5}$$

where $g_i(x_i,\mu^2)$ is the gluon parton density function for hadron i and $\Sigma_i(x_i,\mu^2)$ is the sum over all quark and antiquark density functions for hadron i.

BFKL pomeron exchange has not yet been implemented in PYTHIA . Strongly interacting colour singlet exchange events approximated by high-t photon exchange. PYTHIA was the main model used for detector corrections. HERWIG was used to estimate the systematic errors due to the model dependence of the corrections. In each case, the colour singlet sample was mixed with the direct and resolved photoproduction sample to fit the measured gap fractions. The PYTHIA high-t photon exchange cross section had to be multiplied by a factor of 1200 to fit the observed gap fractions, whilst the normalisation of the HERWIG BFKL pomeron exchange sample was approximately correct. This will be discussed further in section 5.

The transverse energy flow around the jet axes predicted by the HERWIG and PYTHIA generators is compared to the uncorrected data in figure 1. PYTHIA gives a good description both inside and outside the jets. HERWIG fails to describe the energy flow outside the jets, as expected since no multiple interactions model was used. Both generators give a good description of all the kinematic variables used in the analysis. The uncorrected x_p^{jets} and x_γ^{jets} distributions, after the selection cuts described in section 4, are compared to the HERWIG and PYTHIA simulations passed through a complete simulation of the H1 detector in figure 2.

4 Event Selection and Kinematic Reconstruction

The data for this analysis were collected with the H1 detector during the 1996 running period, when HERA collided 27.6 GeV positrons with 820 GeV protons, with an integrated luminosity of 6.2 pb^{-1}. Photoproduction events were selected by detecting the scattered positron in the electron tagger of the luminosity system. This restricts the virtuality of the photon to $Q^2 < 0.01$ GeV^2. The photon-proton centre of mass energy is restricted to the range $165 < W < 233$ GeV to avoid regions of low electron tagger acceptance.

[3]The code can be obtained on request from `coxb@mail.desy.de`.

[4]Note that there is no reason why these 2 parameters should take the same value

The events were triggered by 2 independent triggers, one based on tracking requirements in the central tracker, the other on transverse electromagnetic energy in the SPACAL calorimeter. The trigger efficiency was greater than 50% in all bins.

The inclusive k_t clustering algorithm [26] was applied to the hadronic final state objects. In this mode, the k_t algorithm combines every object in the event uniquely into one and only one jet. The algorithm was run in the 'covariant pt-scheme' with the R parameter set to 1. Objects are defined using a combination of tracking and calorimetric information. Events with 2 or more jets identified by the above algorithm were kept if the two highest E_t jets in the event satisfied the following criteria:

$$E_t^{jet1} > 6.0 \text{ GeV} \tag{6}$$
$$E_t^{jet2} > 5.0 \text{ GeV} \tag{7}$$
$$|\eta^{jet1}, \eta^{jet2}| < 2.8 \tag{8}$$
$$\Delta\eta > 2.5 \tag{9}$$

The first two cuts are asymmetric in order to facilitate comparison with NLO QCD calculations, when such calculations become available. The third cut ensures that the most forward jet (defined at HERA to be the direction of the outgoing proton) is well contained within the LAr calorimeter. The fourth cut ensures a large jet-jet separation, $\Delta\eta = |\eta^{jet1} - \eta^{jet2}|$.

The total transverse energy between the jets, $\not{E}_t^{jets}$, is defined as the sum of the energy of all jets (hereafter referred to as minijets) between the axes of the two highest E_t jets, i.e.

$$\not{E}_t^{jets} = \sum E_t^{minijets} \quad , \quad \eta_{forward}^{jet} > \eta_{minijet} > \eta_{backward}^{jet} \tag{10}$$

A rapidity gap event is defined as an event in which $\not{E}_t^{jets} < E_t^{cut}$, where E_t^{cut} is varied between 0.5 GeV and 5.0 GeV. Such a definition has the advantage of being completely infra-red safe, and relatively insensitive to hadronisation effects. Details can be found in [25].

In addition to the kinematic variables defined above, two scaling variables x_γ^{jets} and x_p^{jets} may be defined, where

$$x_\gamma^{jets} = \frac{\sum_{jets1,2} (E^{jet} - p_z^{jet})}{\sum_{objects} (E^{obj} - p_z^{obj})} \tag{11}$$
$$x_p^{jets} = \frac{\sum_{jets1,2} (E^{jet} + p_z^{jet})}{2E_p} \tag{12}$$

where E_p is the energy of the incoming proton and the sum in the denominator of the x_γ^{jets} calculation is over all objects in the event. x_γ^{jets} and x_p^{jets} are approximately equal to the true x_γ and x_p for leading order jet production.

5 Results and Model Comparisons

The PYTHIA Monte Carlo sample described above was used to correct the data for losses and bin migration effects. The data was also corrected using the HERWIG sample, and the difference assigned as a systematic error. The dijet cross sections for the gap and non-gap samples as measured for different choices of E_t^{cut} are shown in figure 3. The dominant systematic error comes from the uncertainty in the hadronic energy scale of the Liquid Argon Calorimeter, and results in an overall normalisation uncertainty of 20%. The gap fraction, defined as the ratio of the gap and inclusive cross sections, is shown in figure 4. Also shown are the predictions of several Monte Carlo models.

- PYTHIA clearly underestimates the observed gap fraction.

- With the addition of an (unphysically large) sample of high-t photon exchange events, PYTHIA is able to describe the gap fraction for all values of E_t^{cut}.

- HERWIG with JIMMY is unable to describe the observed gap fraction, although the predicted gap fraction is significantly higher than that from PYTHIA at low values of E_T^{cut}.

- With the addition of the BFKL sample a reasonably good description is obtained in the low E_T^{cut} range, although with this choice of parameters the prediction still marginally undershoots the data.

The fact that the HERWIG + JIMMY + BFKL sample describes the data well is a significant observation, since the normalisation of the BFKL sample was not fitted to the data, but resulted from the reasonable choice of $\alpha_s = 0.17$ in equations 1 and 2. At high values of E_t^{cut}, the HERWIG + JIMMY prediction flattens out and even with the addition of the BFKL sample undershoots the data. The behaviour of the gap fraction over the whole E_t^{cut} range was found to be critically dependent on the p_t^{mi} parameter which controls the multiple interactions model in JIMMY . Figure 5 shows the range in the predictions of the gap fraction from HERWIG + JIMMY when p_t^{mi} is varied between 1.7 GeV and 1.9 GeV [5]. The large variation translates into a large uncertainty in the absolute normalisation of the colour singlet sample which must be added to the standard γp processes to fit the data. High-t photon exchange is of course not a candidate for the gap creation mechanism since the cross section is far too low, being suppressed by α_{em}^2.

The gap fraction, differential in $\Delta\eta$, is shown in figure 6 for $E_t^{cut} = 0.5, 1.0, 1.5$ and 2.0 GeV. Again, a significant excess is visible for all values of E_t^{cut} shown in the large $\Delta\eta$ bins, over the predictions from the Monte Carlos without colour-singlet exchange. PYTHIA with high-t photon exchange and HERWIG with JIMMY + BFKL are able to describe the shape of the data distributions equally well.

The gap fraction, differential in x_p^{jets}, is shown in figure 7 for $E_t^{cut} = 0.5, 1.0, 1.5$ and 2.0 GeV. Again, a significant excess is visible for all values of E_t^{cut}, in all x_p^{jets} bins. This time, however, there is a difference between the HERWIG with JIMMY + BFKL and PYTHIA + high-t photon exchange predictions. The high-t photon gap fraction clearly rises with increasing x_p^{jets}, whilst the BFKL sample is flat or falling. This can be understood since a t channel photon can only couple to quarks in the colliding hadrons, whilst the BFKL pomeron, as a gluon dominated object, couples more strongly to gluons than to quarks due to the enhanced colour factors (see equation (5)). The data slightly favour a colour singlet which couples more strongly to gluons.

The gap fraction, differential in x_γ^{jets}, is shown in figure 8 for $E_t^{cut} = 0.5, 1.0, 1.5$ and 2.0 GeV. There is a large excess over the standard γP predictions at low values of E_t^{cut} , and both the HERWIG with JIMMY + BFKL and PYTHIA + high-t photon exchange predictions fit the shape of the data distributions equally well. Note that the standard photoproduction sample is peaked at high x_γ^{jets}, whilst the colour singlet samples are distributed across the whole range. This is due to the fact that direct photoproduction events are much more likely to fluctuate into gap events, since they are purely made up of t-channel quark exchange diagrams. The dominant diagram in resolved events in this kinematic range is gluon-gluon scattering, i.e. t-channel gluon exchange. Even without multiple interactions, which only occur in the resolved process, there is a greatly enhanced probability to emit radiation into the region between the struck partons. Resolved events are consequently very unlikely to produce rapidity gaps at low values of E_t^{cut}.

[5] Generating with $p_t^{mi} = 1.7$ GeV was found to overestimate the energy flow outside the jets as seen in the data (figure 1), whilst $p_t^{mi} = 1.9$ underestimated the energy flow

6 Discussion and Conclusions

It has been shown that there is a significant excess of dijet events with low energy flow between the jets over that predicted by standard photoproduction models. With the exception of the gap fraction differential in x_p^{jets}, the data distributions do not allow conclusions to be drawn on the underlying dynamics of the gap formation process, since a model which couples only to quarks gives similar results to a model which couples primarily to gluons. The BFKL pomeron cross section is of the right order of magnitude for the choice of $\alpha_s = 0.17$. Such a choice was also found to fit the Tevatron gaps between jets data [8], for which the transverse enery of the jets is considerably larger. The reasons for this are as yet unclear; equation 1 has been derived using the leading logarithmic approximation of BFKL, and the higher order corrections at non-zero t are unknown at present. Even within the LLA, there are large uncertainties due to the choice of scales and the treatment of the running coupling (which has been treated as a fixed parameter in this analysis). A further complication is introduced by the issue of rapidity gap survival; BFKL events will not all lead to rapidity gaps. The normalisation of the BFKL cross section must take this into account, and this has not been considered here. Estimates of the gap survival probability at HERA are quite high, however. In reference [8], for example, the gap survival probability was estimated to be as high as $\sim 70\%$ in γp collisions. A final complication arises because of the uncertainty in the knowledge of the gap formation probability in the standard photoproduction processes. The prediction from PYTHIA is very much lower than that from HERWIG + JIMMY . Further, even within a particular model, the gap formation probability is critically dependent upon the choice of p_t^{mi}, as shown in figure 5. With these caveats the BFKL model of [7] is consistant with the data.

The gap fraction as a function of x_p^{jets} does exhibit some sensitivity to the colour singlet model used, and favours a gap production mechanism which creates more gaps in gluon initiated events. This favours 2-gluon based perturbative models of colour singlet exchange such as the BFKL pomeron, and disfavours soft-colour type models. Soft-colour models predict that quark initiated events produce more gaps since quarks have less colour states than gluons, and hence the probability for a fluctuation into a colour singlet configuration is higher.

7 Acknowledgments

We are grateful to the HERA machine group whose outstanding efforts have made and continue to make this experiment possible. We thank the engineers and technicians for their work in constructing and now maintaining the H1 detector, our funding agencies for financial support, the DESY technical staff for continual assistance, and the DESY directorate for the hospitality which they extend to the non-DESY members of the collaboration.

References

[1] H1 Collaboration: C.Adloff et al., Z.Phys. C74 (1997) 221.

[2] S. Abachi et al (D0 collaboration), Phys. Rev. Lett. 72 (1994) 2332; Phys. Rev. Lett. 76 (1996) 734; B. Abbott et al (D0 collaboration), Phys. Lett. B440 (1998) 189.

[3] F. Abe et al (CDF collaboration), Phys. Rev. Lett. 74 (1995) 855; Phys. Rev. Lett 80 (1998) 1156; Phys. Rev. Lett. 81 (1998) 5278.

[4] M. Derrick et al (ZEUS collaboration), Phys. Lett. B369 (1996) 55.

[5] J.R.Forshaw and P.J.Sutton, Eur.Phys.J. C1 (1998) 285.

[6] E.A.Kuraev, L.N.Lipatov and V.S.Fadin, Sov.Phys.JETP 45 (1977) 199.
Ya.Ya.Balitsky and L.N.Lipatov, Sov.J.Nucl.Phys 28 (1978) 822.
L.N.Lipatov, Sov.Phys.JETP 63 (1986) 904.

[7] A.H.Mueller and W.-K.Tang, Phys.Lett. B284, (1992) 123.

[8] B.E.Cox, J.R. Forshaw, L.Lönnblad, JHEP10(1999)023.

[9] H1 Collaboration, "Production of J/ψ Mesons with large $|t|$ at HERA", contribution to the International Europhysics Conference on High Energy Physics, Jerusalem, Israel (1997).

[10] J. Crittenden, "Recent Results from Decay-Angle Analyses of ρ^0 Photoproduction at High Momentum Transfer from ZEUS", contribution to the DIS99 Workshop, Zeuthen, Germany (1999) `hep-ex/9906005`.

[11] J. D. Bjorken, Phys. Rev. **D47** (1993) 101.

[12] E.Gotsman, E.Levin, U.Maor, Phys. Lett. B438 (1998) 229; Phys. Rev. D60 (1999)

[13] G. Oderda and G. Sterman, Phys. Rev. Lett. 81, 3591 (1998).

[14] G. Oderda, Stony Brook report ITP-SB-98-70, March 1999, hep-ph/9903240.

[15] O.J.P. Éboli, E. M. Gregores, F. Halzen, Phys. Rev. D. 58, (1998), 114005; hep-ph/9908374.

[16] H1 Collaboration; I. Abt et al., Nucl. Instr. and Meth. **A386** (1997) 310; 348.

[17] H1 Calorimeter Group; B. Andrieu et al., Nucl. Instr. and Meth. **A336** (1993) 460.

[18] H1 SPACAL group, R.D. Appuhn et al., Nucl. Instr. and Meth. **A386** (1997) 397.

[19] T. Sjöstrand and M. van Zijl, Phys. Rev. **D36** (1987) 2019

[20] G.Marchesini et al., Comp.Phys.Comm. 67 (1992) 465.

[21] M.E.Hayes, Bristol University, PhD Thesis (1998).

[22] H1 Collaboration: DESY-98-205

[23] J. M. Butterworth, J. R. Forshaw and M. H. Seymour, Z. Phys. **C72** (1996) 637-646.

[24] M. Glück, E. Reya, A. Vogt, Z. Phys. **C67** (1995) 433.

[25] B. E. Cox, M. H. Seymour and A. C. Wyatt, in preparation.

[26] S. D. Ellis and D. E. Soper, Phys. Rev. **D48** (1993) 3160.

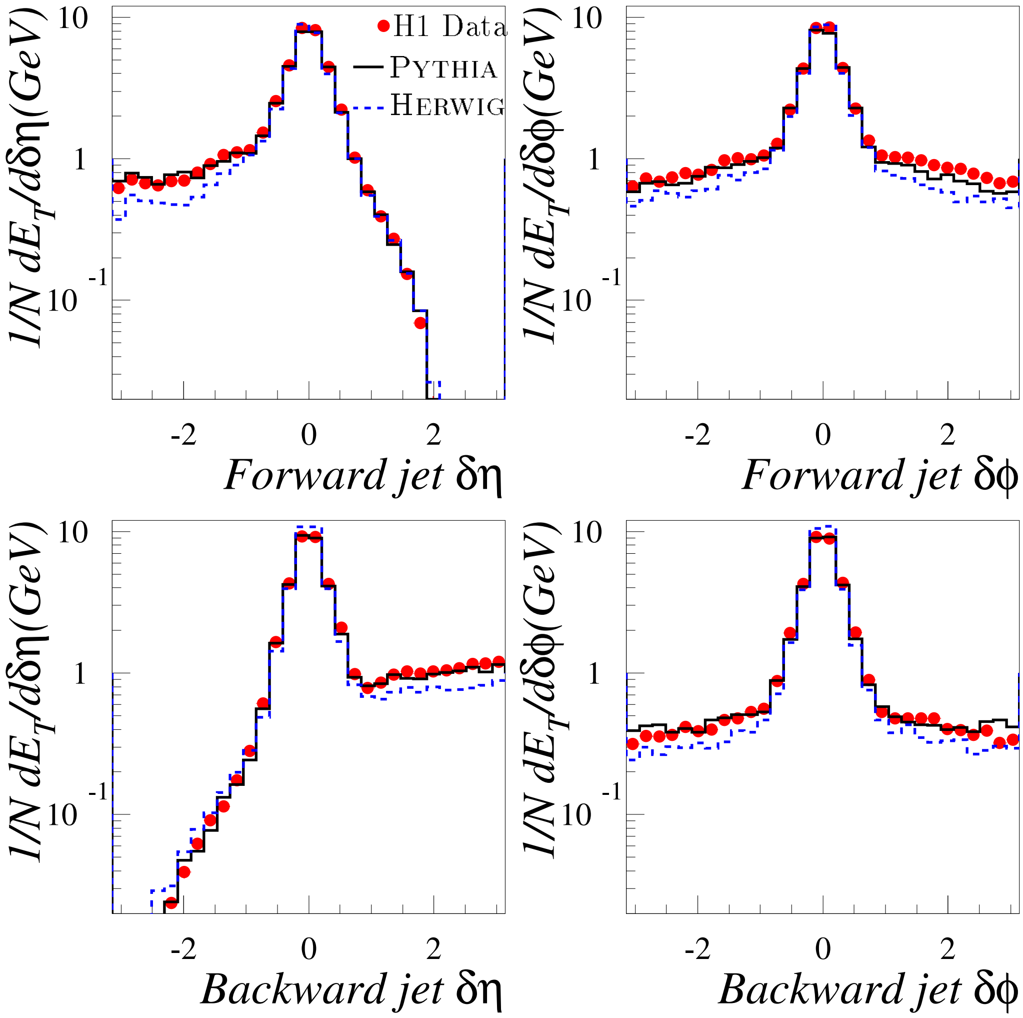

Figure 1: Jet profiles for the forward (proton direction) and backward jets. H1 data are shown as points. The solid histogram is the prediction of the PYTHIA simulation, and the dashed histogram that of HERWIG

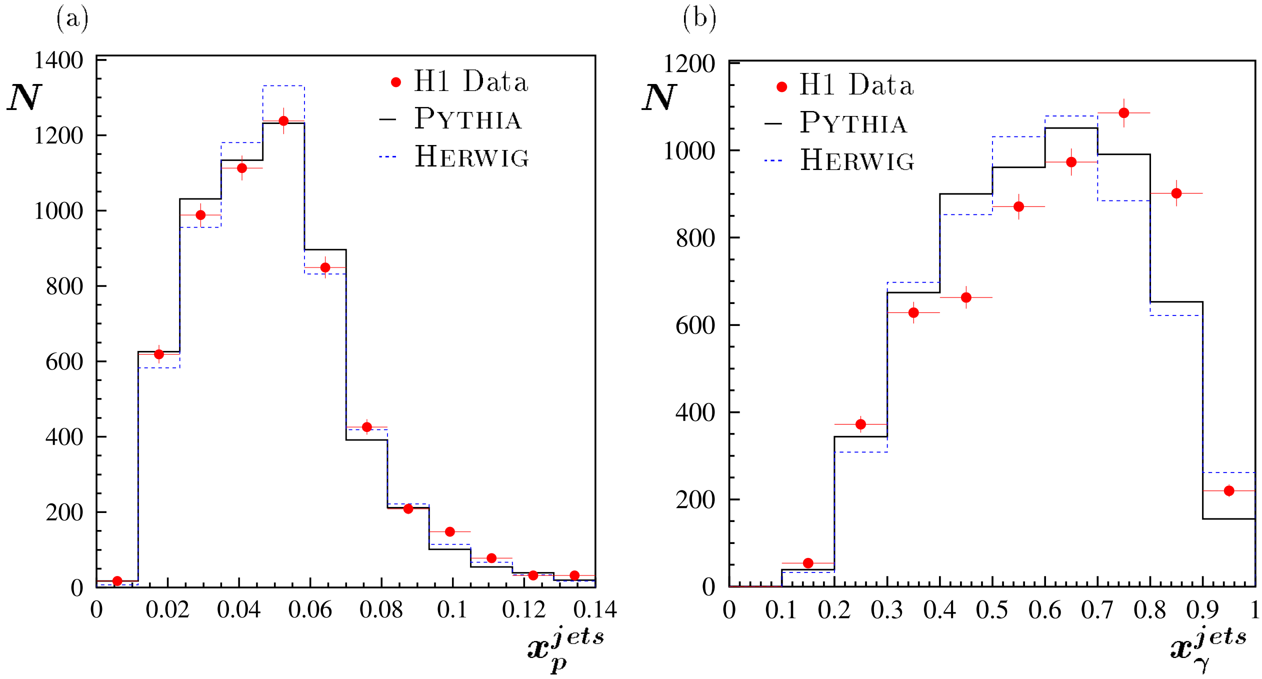

Figure 2: Figure (a) shows the x_p^{jets} distribution in the kinematic range defined by the cuts in section 4. Figure (b) shows the x_γ^{jets} distribution in the same kinematic range. The uncorrected data are shown as solid points. The solid histogram is the prediction of the PYTHIA simultaion, and the dashed histogram that of HERWIG

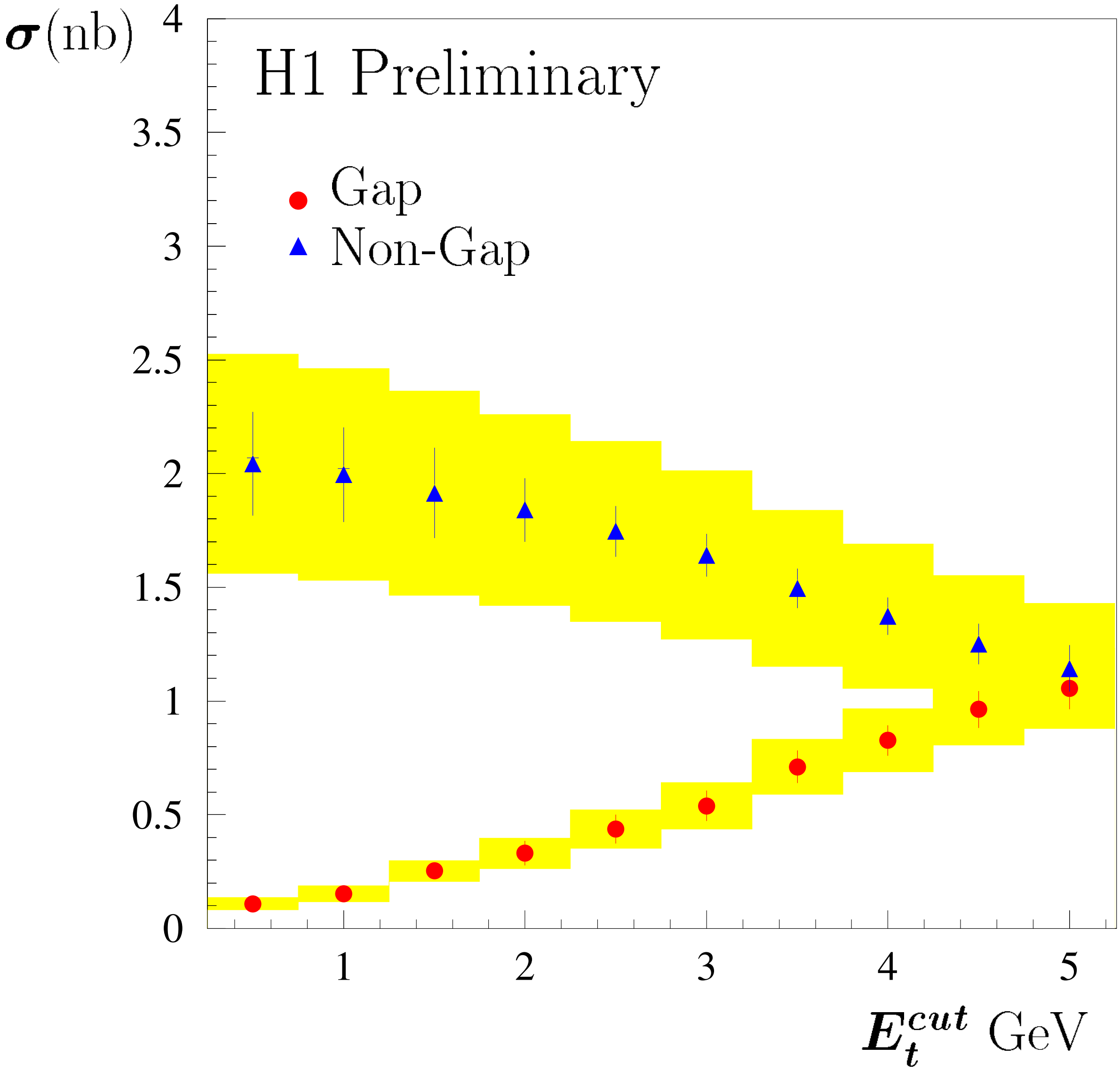

Figure 3: The dijet cross section in the kinematic range defined in section 4. The solid circles show the gap cross section for different choices of E_t^{cut}, and the solid triangles show the non-gap cross section. The inner error bars show the statistical errors, and the outer error bars show the sum of the statistical and systematics errors added in quadrature. The solid band shows the correlated systematic error, which is dominated by the uncertainty in the knowledge of the Calorimeter energy scale. It should be noted that the data-points themselves are highly correlated in this plot

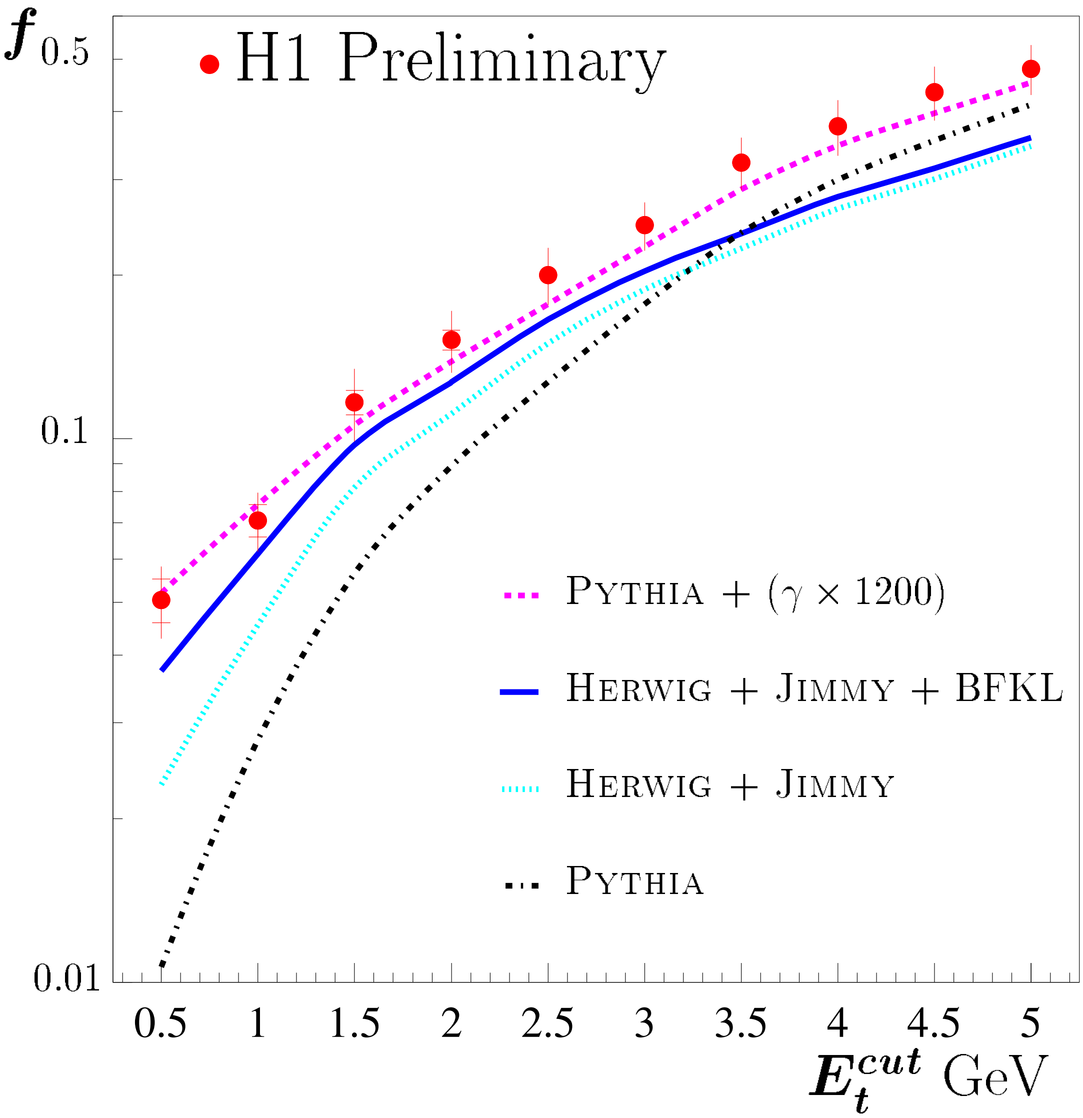

Figure 4: The gap fraction as the energy cut E_t^{cut} used to define a gap is varied between 0.5 GeV and 5.0 GeV, compared to different Monte Carlo models. Herwig + BFKL is a HERWIG 5.9 + Jimmy photoproduction sample with BFKL colour singlet exchange added according to the predicted cross section with $\alpha_s = 0.17$ [7]. PYTHIA + ($\gamma \times 1200$) is a PYTHIA photoproduction sample with high$-t$ photon exchange added, with the generated cross section multiplied by a factor of 1200. Also shown are HERWIG 5.9 + Jimmy and PYTHIA 5.7 photoproduction samples with no colour singlet component added.

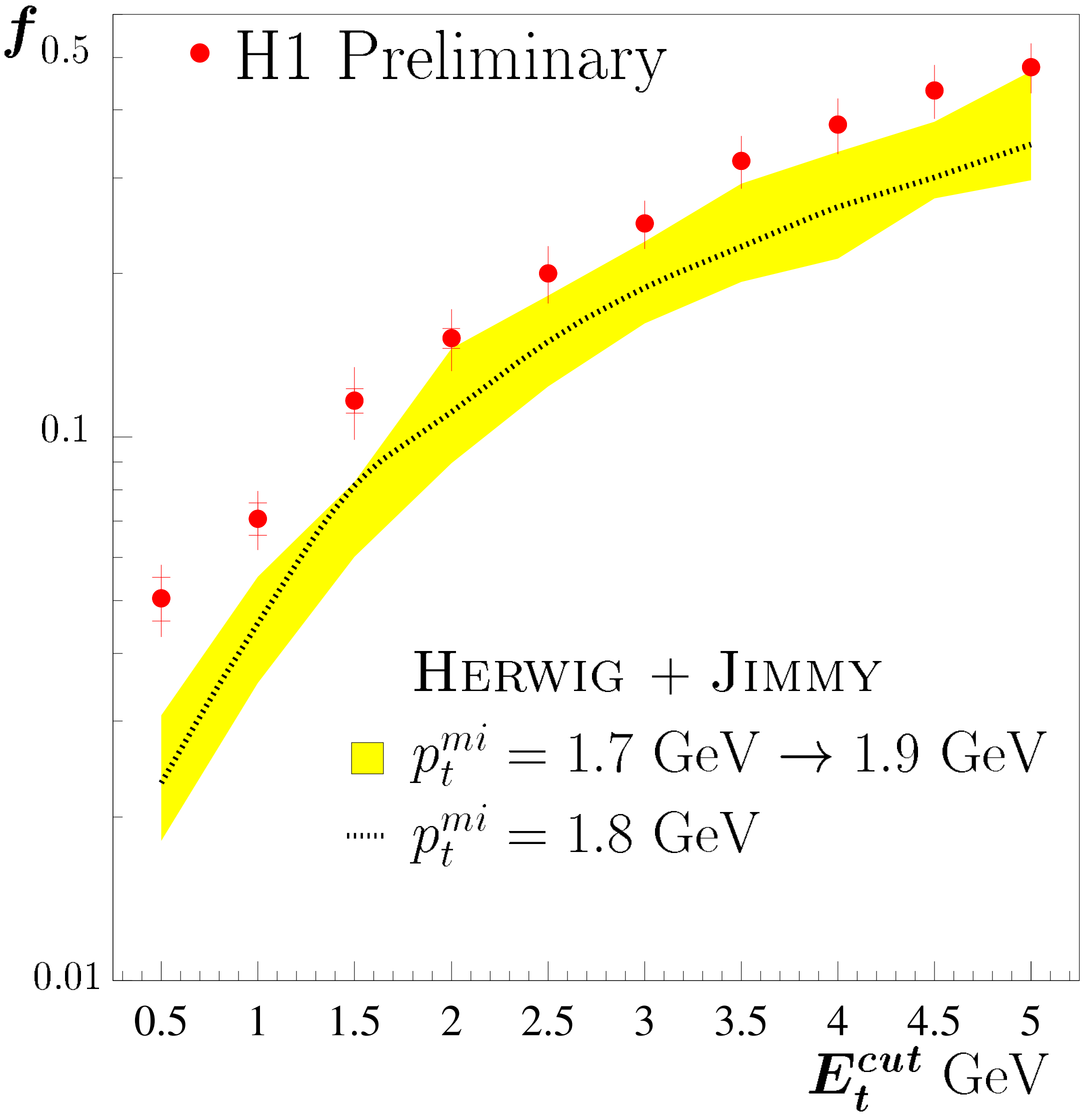

Figure 5: The gap fraction as the energy cut E_t^{cut} used to define a gap is varied between 0.5 GeV and 5.0 GeV. The solid band shows the variation in the HERWIG + JIMMY prediction as the minimum p_t at which multiple hard scatters are allowed to take place, p_t^{mi}, is varied between 1.7 GeV and 1.9 GeV.

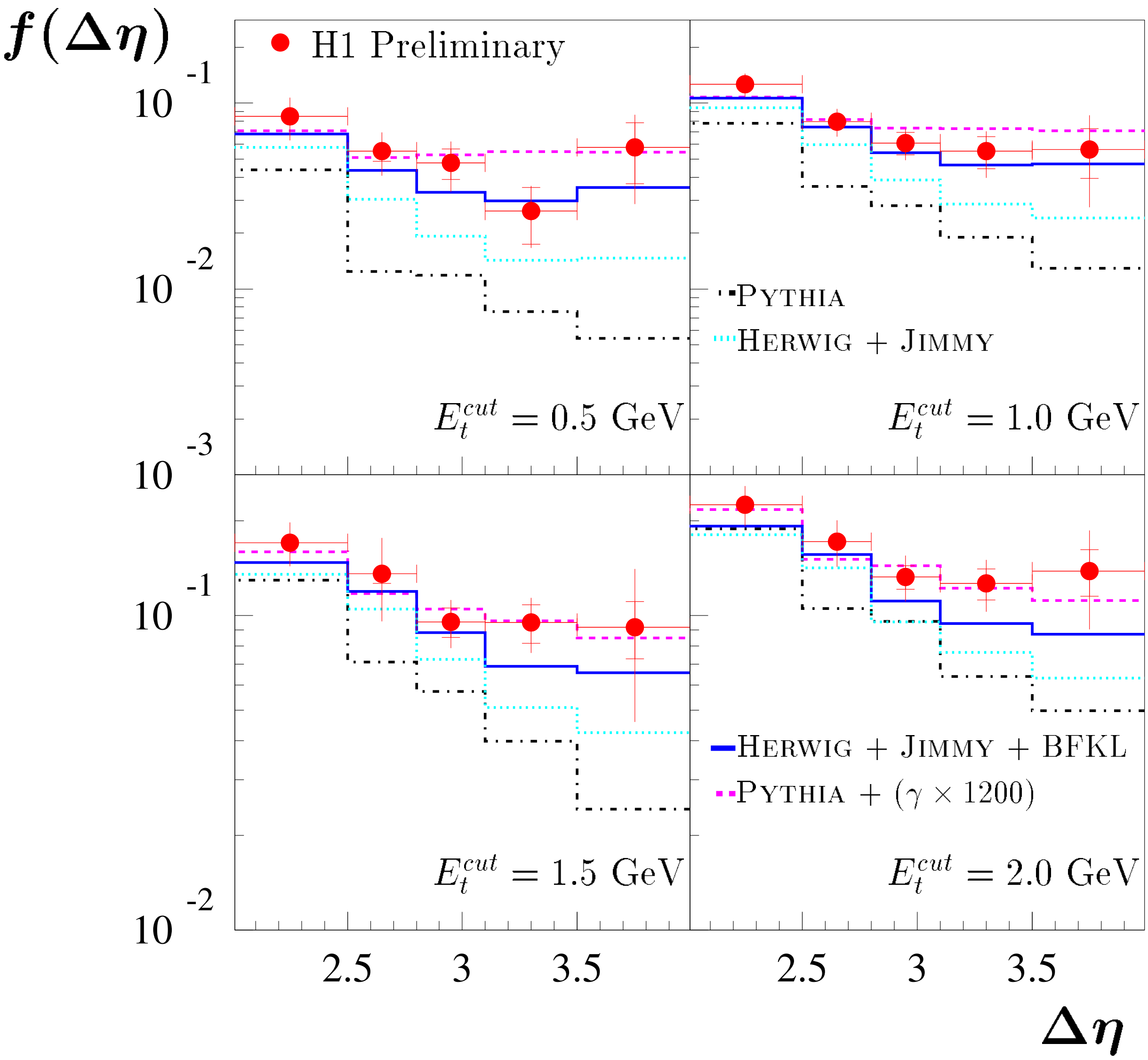

Figure 6: The gap fraction differential in $\Delta\eta$ for $E_t^{cut} = 0.5, 1.0, 1.5, 2.0$ GeV , compared to different Monte Carlo models. Herwig + BFKL is a HERWIG 5.9 + Jimmy photoproduction sample with BFKL colour singlet exchange added according to the predicted cross section with $\alpha_s = 0.17$ [7]. PYTHIA + $(\gamma \times 1200)$ is a PYTHIA photoproduction sample with high$-t$ photon exchange added, with the generated cross section multiplied by a factor of 1200. Also shown are HERWIG 5.9 + Jimmy and PYTHIA 5.7 photoproduction samples with no colour singlet component added.

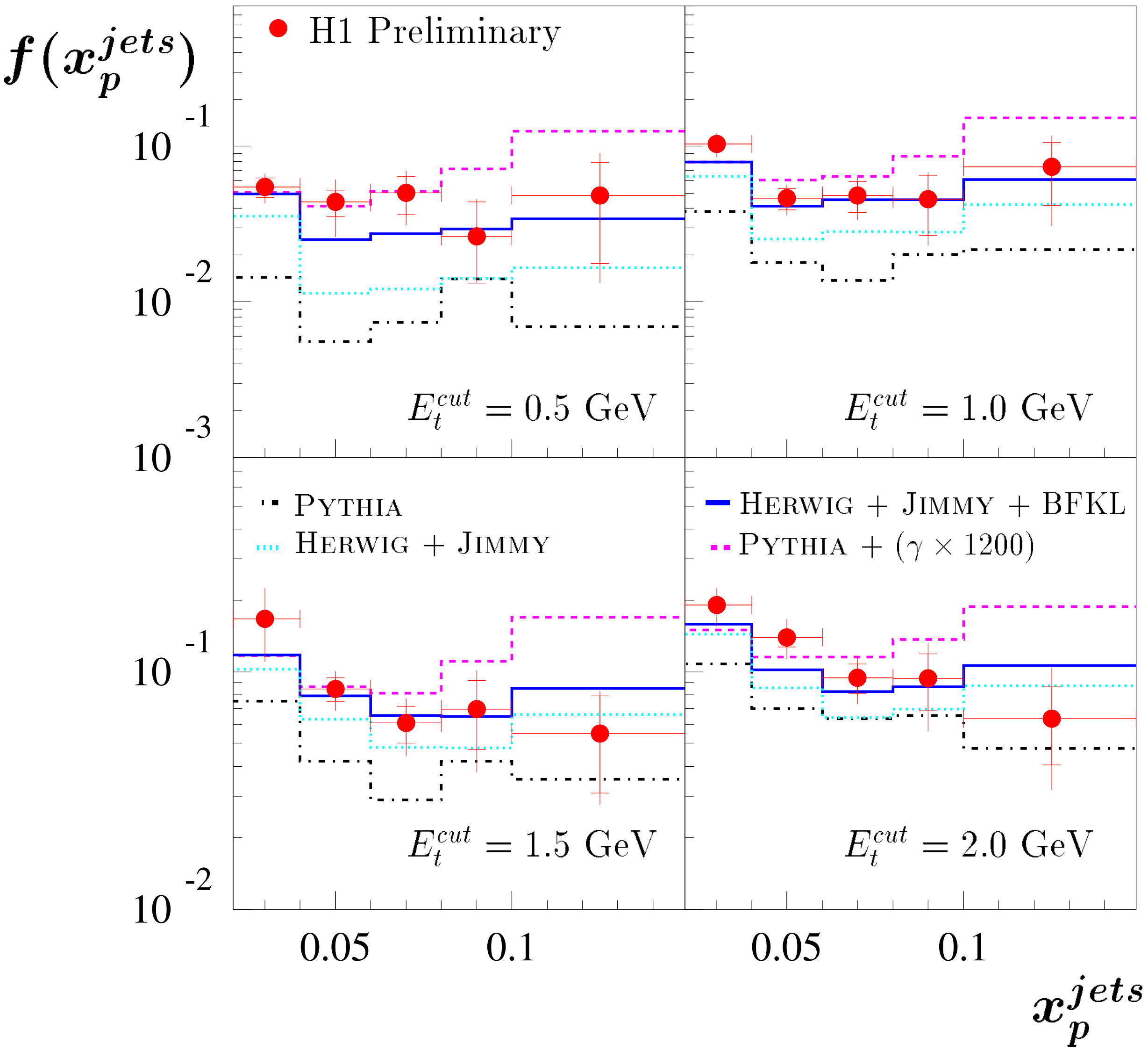

Figure 7: The gap fraction differential in x_p^{jets} for $E_t^{cut} = 0.5, 1.0, 1.5, 2.0$ GeV , compared to different Monte Carlo models. Herwig + BFKL is a HERWIG 5.9 + Jimmy photoproduction sample with BFKL colour singlet exchange added according to the predicted cross section with $\alpha_s = 0.17$ [7]. PYTHIA + ($\gamma \times 1200$) is a PYTHIA photoproduction sample with high$-t$ photon exchange added, with the generated cross section multiplied by a factor of 1200. Also shown are HERWIG 5.9 + Jimmy and PYTHIA 5.7 photoproduction samples with no colour singlet component added.

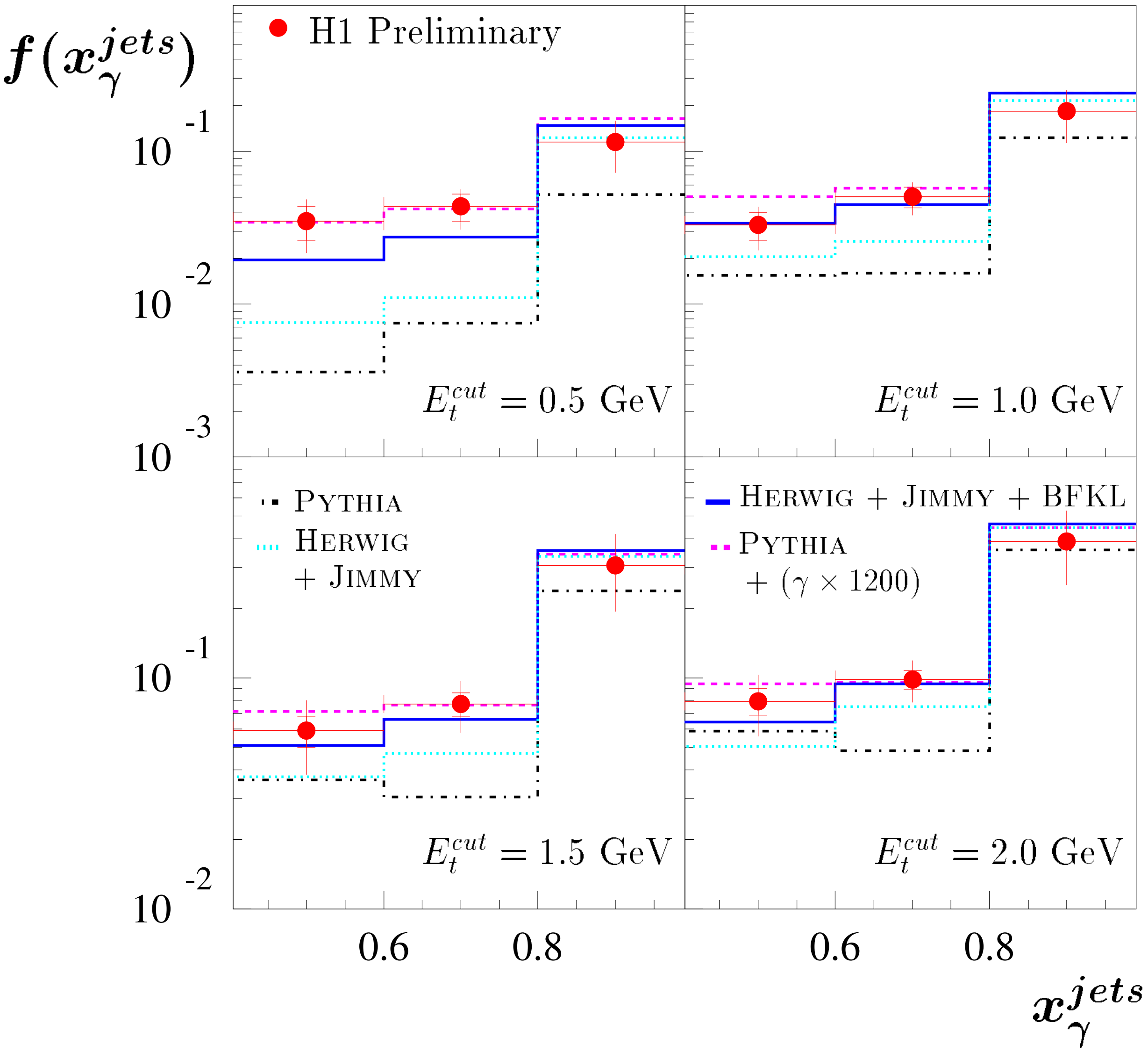

Figure 8: The gap fraction differential in x_γ^{jets} for $E_t^{cut} = 0.5, 1.0, 1.5, 2.0$ GeV , compared to different Monte Carlo models. Herwig + BFKL is a HERWIG 5.9 + Jimmy photoproduction sample with BFKL colour singlet exchange added according to the predicted cross section with $\alpha_s = 0.17$ [7]. PYTHIA + ($\gamma \times 1200$) is a PYTHIA photoproduction sample with high$-t$ photon exchange added, with the generated cross section multiplied by a factor of 1200. Also shown are HERWIG 5.9 + Jimmy and PYTHIA 5.7 photoproduction samples with no colour singlet component added.